

Effects of nonthermal distribution of electrons and polarity of net dust-charge number density on nonplanar dust-ion-acoustic solitary waves

A. A. Mamun* and P. K. Shukla

Fakultät für Physik und Astronomie, Ruhr-Universität Bochum, D-44780 Bochum, Germany

(Received 17 June 2009; revised manuscript received 31 August 2009; published 25 September 2009)

Effects of the nonthermal distribution of electrons as well as the polarity of the net dust-charge number density on nonplanar (viz. cylindrical and spherical) dust-ion-acoustic solitary waves (DIASWs) are investigated by employing the reductive perturbation method. It is found that the basic features of the DIASWs are significantly modified by the effects of nonthermal electron distribution, polarity of net dust-charge number density, and nonplanar geometry. The implications of our results in some space and laboratory dusty plasma environments are briefly discussed.

DOI: [10.1103/PhysRevE.80.037401](https://doi.org/10.1103/PhysRevE.80.037401)

PACS number(s): 52.27.Lw

Shukla and Silin [1] theoretically showed that due to the conservation of equilibrium charge density $n_{e0} + z_n n_n = n_{i0}$ and the strong inequality $n_{e0} \ll n_{i0}$ [where n_{e0} (n_{i0}) is the equilibrium electron (ion) number density, n_n is the equilibrium number density of negatively charged dust (negative dust), z_n is the number of electrons residing onto the negative-dust grain surface, and e is the magnitude of the electron charge], a dusty plasma with stationary negative-dust supports low-frequency dust-ion-acoustic (DIA) waves (DIAs) with phase speed much smaller (larger) than the electron (ion) thermal speed. The DIAs have also been observed in laboratory experiments [2,3]. The linear properties of DIAs in dusty plasmas are now well understood from both theoretical [1,4,5] and experimental [2–4] points of view. The nonlinear propagation of DIAs have also received a great deal of interest in understanding the features of localized electrostatic perturbations in space and laboratory dusty plasmas [6–13].

On the other hand, it has been found from both experimental observation [14,15] and theoretical analysis [16,17] that the presence of nonthermal (fast) electrons, which occur in many space plasma situations, particularly, in upper part of ionosphere or lower part of magnetosphere [14,15], significantly modifies the basic features of ion-acoustic solitary waves (IASWs) or introduces new features in them. A limited number of theoretical investigations (e.g., Tribeche and Berbri [18] and Xue [19]) has been made on DIASWs in dusty plasma containing negative-dust inertial ions and nonthermal electrons. Tribeche and Berbri [18] extended the work of Mamun and Shukla [13] to include the effects of nonthermal electron distribution on one-dimensional (1D) planar DIA solitary and shock waves. Xue [19] considered nonplanar cylindrical and spherical geometries and examined the interaction between the compressive and rarefactive DIASWs.

It has also been found that in some of the space environments (viz. upper part of ionosphere or lower part of magnetosphere, where dust number density varies from ~ 10 to $\sim 100 \text{ cm}^{-3}$ and dust size varies from ~ 0.1 to $\sim 1 \text{ }\mu\text{m}$),

dust are positively charged [20–22] though in most space and laboratory dusty plasma environments dust are negatively charged [23,24]. It has been also observed that in some of these space environments, particularly, in mesopause dust of opposite polarity [i.e., positively charged dust (positive dust) as well as negatively charged dust (negative dust)] exist [25]. Therefore, in this Brief Report, we consider a more general dusty plasma system containing electrons following nonthermal distribution of Cairns *et al.* [16], inertial ions, stationary dust of opposite polarity (positive-dust as well as negative-dust), and study the nonplanar (cylindrical and spherical) DIASWs in such a dusty plasma.

We consider a more general unmagnetized dusty plasma system, whose constituents are nonthermal electrons, inertial ions, and stationary dust of opposite polarity (i.e., positive as well as negative dust). The nonlinear dynamics of nonplanar (cylindrical and spherical) DIAs propagating in such a dusty plasma with phase speed much smaller (larger) than the electron (ion) thermal speed is governed by

$$\frac{\partial n_i}{\partial t} + \frac{1}{r^\nu} \frac{\partial}{\partial r} (r^\nu n_i u_i) = 0, \quad (1)$$

$$\frac{\partial u_i}{\partial t} + u_i \frac{\partial u_i}{\partial r} = - \frac{\partial \phi}{\partial r}, \quad (2)$$

$$\frac{1}{r^\nu} \frac{\partial}{\partial r} \left(r^\nu \frac{\partial \phi}{\partial r} \right) = (1 + s\delta)n_e - n_i - s\delta, \quad (3)$$

where $\nu=0$ for 1D planar geometry and $\nu=1(2)$ for a nonplanar cylindrical (spherical) geometry, n_i is the ion number density normalized by its equilibrium value n_{i0} , u_i is the ion fluid speed normalized by the ion-acoustic speed $C_i = (T_e/m_i)^{1/2}$, ϕ is the electrostatic wave potential normalized by T_e/e , n_e is the electron number density normalized by its equilibrium value n_{e0} , $\delta = |z_p n_p - z_n n_n|/n_{i0}$, s represents the polarity of the net dust-charge number density (i.e., $s=1$ for $z_p n_p > z_n n_n$ and $s=-1$ for $z_p n_p < z_n n_n$), n_p is the positive dust number density at equilibrium, z_p is the number of excess protons residing on a positive-dust grain surface, T_e is the electron temperature in units of the Boltzmann constant, and m_i is the ion mass. The time and space variables are in units

*Permanent address: Department of Physics, Jahangirnagar University, Savar, Dhaka 1342, Bangladesh.

of the ion plasma period $\omega_{pi}^{-1} = (m_i/4\pi n_{i0}e^2)^{1/2}$, and the Debye radius $\lambda_{Dm} = (T_e/4\pi n_{i0}e^2)^{1/2}$, respectively. At equilibrium, we have $n_{i0} + z_p n_p = n_{e0} + z_n n_n$. It is obvious that (i) for $s=1$ and $z_n=0$, Eqs. (1)–(3) represent a dusty plasma with positive dust where $\delta = z_p n_p / n_{i0}$, (ii) for $s=-1$ and $z_p=0$, Eqs. (1)–(3) represent a dusty plasma with negative dust where $\delta = z_n n_n / n_{i0}$, and (iii) for $z_p \neq 0$ and $z_n \neq 0$, Eqs. (1)–(3) represent a dusty plasma with the coexistence of positive and negative dusts where $\delta = |z_p n_p - z_n n_n| / n_{i0}$ and $s=1$ ($z_p n_p > z_n n_n$) or $s=-1$ ($z_p n_p < z_n n_n$). We note that we have assumed spherical or cylindrical symmetry since we are interested in radial propagation of the nonlinear DIAWs.

We assume that electrons follow the nonthermal distribution [16]:

$$f_e(v) = \frac{n_{e0}}{(1+3\alpha)\sqrt{2\pi V_{Te}^2}} \left(1 + \frac{\alpha v^4}{V_{Te}^4}\right) \exp\left(-\frac{v^2}{2V_{Te}^2}\right),$$

where V_{Te} is the electron thermal speed and α is the parameter determining the number of nonthermal electrons present in our nonthermal dusty plasma model [16,17]. We note that α is always less than 1, i.e., $0 \leq \alpha < 1$, and that $\alpha=0$ corresponds to the Boltzmann distribution of electrons. Thus, the normalized electron number density n_e corresponding to this nonthermal distribution [16] is given by [16,17]

$$n_e = \left[1 - \frac{4\alpha\phi}{1+3\alpha}(1-\phi)\right] \exp(\phi). \quad (4)$$

To derive a dynamical equation for the nonlinear propagation of the DIAWs from Eqs. (1)–(4) by using the reductive perturbation technique, we introduce the stretched coordinates [26]:

$$\zeta = -\epsilon^{1/2}(r + V_p t), \quad \tau = \epsilon^{3/2} t, \quad (5)$$

expand n_i , u_i , and ϕ in a power series of ϵ :

$$n_i = 1 + \epsilon n_i^{(1)} + \epsilon^2 n_i^{(2)} + \dots, \quad (6)$$

$$u_i = 0 + \epsilon u_i^{(1)} + \epsilon^2 u_i^{(2)} + \dots, \quad (7)$$

$$\phi = 0 + \epsilon \phi^{(1)} + \epsilon^2 \phi^{(2)} + \dots, \quad (8)$$

and develop equations in various powers of ϵ . To the lowest order in ϵ , Eqs. (1)–(8) give

$$n_i^{(1)} = -\frac{u_i^{(1)}}{V_p} = \frac{\phi^{(1)}}{V_p^2}, \quad (9)$$

$$V_p = \left[\frac{1+3\alpha}{(1-\alpha)(1+s\delta)} \right]^{1/2}, \quad (10)$$

where V_p is the DIAW phase speed normalized by C_i and Eq. (10) represents the linear dispersion relation for the DIAWs under consideration. It is obvious that the phase speed is significantly increased by the presence of nonthermal electrons and that it is decreased when the net dust-charge number density is positive ($s=1$), but it is increased when the net dust-charge number density is negative ($s=-1$).

To the next higher order in ϵ , we obtain three coupled equations for $n_i^{(2)}$, $u_i^{(2)}$, and $\phi^{(2)}$. Now, using Eqs. (9) and

(10), one can combine these three coupled equations and can finally obtain a nonlinear dynamical equation for the DIAWs:

$$\frac{\partial \Psi}{\partial \tau} + \frac{\nu}{2\tau} \Psi + A \Psi \frac{\partial \Psi}{\partial \zeta} + B \frac{\partial^3 \Psi}{\partial \zeta^3} = 0, \quad (11)$$

where $\Psi = \phi^{(1)}$ and

$$A = B(1+s\delta) \left[3(1+s\delta) \frac{(1-\alpha)^2}{(1+3\alpha)^2} - 1 \right], \quad (12)$$

$$B = \frac{1}{2} \left[\frac{1+3\alpha}{(1-\alpha)(1+s\delta)} \right]^{3/2}. \quad (13)$$

Equation (11) is a modified Korteweg–de Vries (mK-dV) equation which includes the effects of nonthermal electrons (through α), polarity of the net dust-charge number density (through s), and nonplanar geometry (through ν). The extra term $(\nu/2\tau)\Psi$ in Eq. (11) is due to the effect of the cylindrical ($\nu=1$) or spherical ($\nu=2$) geometry.

We note that if we consider a dusty plasma with negative dust ($z_p=0$ and $s=-1$) and 1D planar geometry ($\nu=0$), our mK-dV Eq. (11) reduces to the K-dV equation (with constant dust-charge assumption) derived by Tribeche and Berbri [18]. However, like other earlier works (viz. Mamun and Shukla [13]), the dissipative coefficient C [Eq. (36)] of the K-dV-Burgers equation derived by Tribeche and Berbri [18] contains the expansion parameter ϵ because of their assumption $\eta = \epsilon^{1/2} \eta_0$, where $\eta = \sqrt{8\pi r_d^2 \lambda_{Dm} n_{i0}}$ according to Tribeche and Berbri [18]. This may not be the correct approach for the study of the DIA shock waves by the reductive perturbation method. On the other hand, if we consider a dusty plasma with negative dust ($z_p=0$ and $s=-1$), our mK-dV Eq. (11) becomes similar to the one of the two coupled equations derived by Xue [19] who studied the interactions of two DIASWs by using the stretched coordinates which are completely different from our ones. The reason of using different stretched coordinates is that the aim of the investigation of Xue [19] is completely different from that of our present work.

The stationary solitary wave solution of Eq. (11) for a 1D planar geometry ($\nu=0$) and for a frame moving with a speed U_0 is

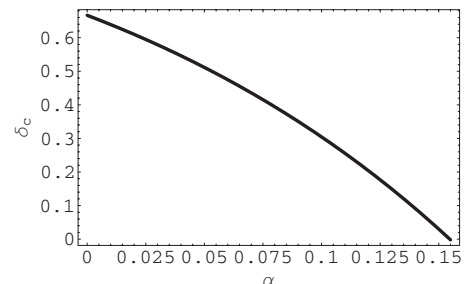


FIG. 1. The variation in δ_c with α for $s=-1$.

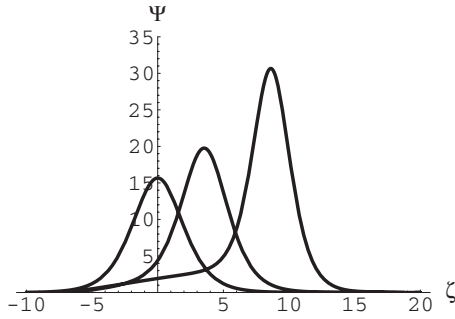


FIG. 2. Time evolution of cylindrical ($\nu=1$) DIASWs at times $\tau=-9$ (left), $\tau=-6$ (middle), and $\tau=-3$ (right) for $s=-1$, $\delta=0.5$, and $\alpha=0.025$.

$$\Psi(\nu=0) = \left(\frac{3U_0}{A}\right) \text{sech}^2 \left[\sqrt{\frac{U_0}{4B}} (\zeta - U_0\tau) \right]. \quad (14)$$

It is obvious from Eqs. (12)–(14) that compressive (rarefactive) DIASWs, which are associated with positive (negative) potential, exist if $A > 0$ ($A < 0$), i.e.,

$$(1 + s\delta) \frac{(1 - \alpha)^2}{(1 + 3\alpha)^2} > (<) \frac{1}{3}. \quad (15)$$

Therefore, the critical value (δ_c) of δ (as a function of α) is given by

$$\delta_c = \frac{1}{s} \left[\frac{(1 + 3\alpha)^2}{3(1 - \alpha)^2} - 1 \right]. \quad (16)$$

We have numerically analyzed how δ_c varies with α for $s = -1$. The numerical results are displayed in Fig. 1.

It is obvious from Fig. 1 that the coexistence of negatively charged dust and nonthermal electrons significantly enhances the possibility for the formation of rarefactive DIASWs, i.e., as negative dust number density is higher, we need lower values of α in order to have rarefactive DIASWs. We can also show by a similar numerical analysis with $s=1$ that the presence of positively charged dust (nonthermal electrons) reduces (enhances) the possibility for the formation of rarefactive DIASWs, i.e., as positive dust number density is higher, we need higher values of α in order to have rarefactive DIASWs.

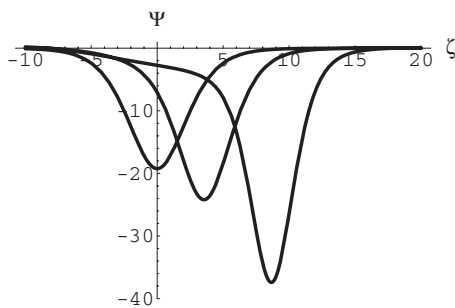


FIG. 3. Time evolution of cylindrical ($\nu=1$) DIASWs at times $\tau=-9$ (left), $\tau=-6$ (middle), and $\tau=-3$ (right) for $s=-1$, $\delta=0.5$, and $\alpha=0.075$.

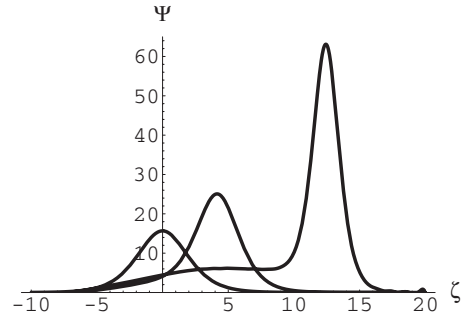


FIG. 4. Time evolution of spherical ($\nu=2$) DIASWs at times $\tau=-9$ (left), $\tau=-6$ (middle), and $\tau=-3$ (right) for $s=-1$, $\delta=0.5$, and $\alpha=0.025$.

We have finally numerically solved Eq. (11) and have studied the effects of cylindrical and spherical geometries on time-dependent DIASWs. The results are depicted in Figs. 2–5. The initial condition used in our numerical analysis is $\Psi = (3U_0/A) \text{sech}^2(\zeta \sqrt{U_0/4B})$, which is the stationary solitary wave solution of Eq. (11) without the term $(\nu/2\tau)\Psi$. We choose our initial pulse at $\tau = -9$ and show how its amplitude increases by decreasing the value of τ . We also use $U_0 = 1$ through out our numerical analysis. Figures 2–5 show how the effects of cylindrical and spherical geometries modify DIASWs in a plasma with the coexistence of dust of opposite polarity (with $s = -1$) and nonthermal electrons. Figure 2 (Fig. 3) shows the time evolution of compressive (rarefactive) cylindrical DIASWs. On the other hand, Fig. 4 (Fig. 5) shows the time evolution of compressive (rarefactive) spherical DIASWs. Figures 2–5 clearly imply that depending on the values of α and δ , we can have either compressive (shown in Figs. 2 and 4) or rarefactive (shown in Figs. 3 and 5) DIASWs and that due to the change in the value of α from 0.025 to 0.075, compressive DIASWs (shown in Figs. 2 and 4) are converted into rarefactive ones (shown in Figs. 3 and 5). By a similar numerical analysis with $s=1$, we can show that depending on the values of α and δ , we can have either compressive or rarefactive DIASWs and that due to the change in the value of α from 0.2 to 0.3, compressive DIASWs are converted into rarefactive ones.

The numerical solutions of Eq. (11) (displayed in Figs. 2–5) reveal that for a large value of τ (e.g., $\tau = -9$) the spherical and cylindrical DIASWs are similar to 1D planar ones. This is because for a large value of τ the term $(\nu/2\tau)\Psi$ is no

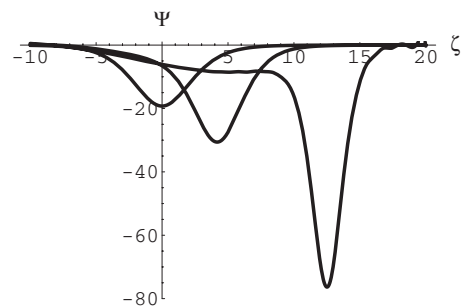


FIG. 5. Time evolution of spherical ($\nu=2$) DIASWs at times $\tau=-9$ (left), $\tau=-6$ (middle), and $\tau=-3$ (right) for $s=-1$ (negative dust), $\delta=0.5$, and $\alpha=0.075$.

longer dominant. However, as the value of τ decreases, the term $(\nu/2\tau)\Psi$ becomes dominant, and both cylindrical and spherical DIASWs differ from 1D planar ones. The numerical solutions of Eq. (11) (displayed in Figs. 2–5) also reveal that the effects of nonthermal electrons and nonplanar (cylindrical and spherical) geometries significantly modify the basic features (amplitude, width, etc.) of the DIASWs and that time evolution of the DIASWs in both cylindrical and spherical geometries are very significant although the effects in spherical geometry are more significant than those in cylindrical geometry. The amplitude of the DIASWs increases with increasing the value of τ . The amplitude of cylindrical DIASWs is larger than that of the 1D planar ones but smaller than that of the spherical ones.

To conclude, DIASWs are more suitable than any other dust associated nonlinear waves to observe in laboratory

dusty plasma experiments. We, therefore, propose to perform a laboratory experiment which will be able to identify such special new features of the DIASWs predicted in this investigation. It has been shown that the refractive IASWs (observed by Freja satellite [15,16]) is because of the presence of nonthermal electrons, and they are formed only when $\alpha > 0.155$ [16]. However, we have predicted in our study that the rarefactive IASWs can be formed for any values of α if negatively charged dust exist there. We, finally, hope that our present results may help to understand the salient features of the DIASWs when data for space and laboratory observations become available.

A.A.M. is grateful to the Alexander von Humboldt Stiftung (Germany) for the financial support.

-
- [1] P. K. Shukla and V. P. Silin, *Phys. Scr.* **45**, 508 (1992).
 [2] A. Barkan, N. D'Angelo, and R. L. Merlino, *Planet. Space Sci.* **44**, 239 (1996).
 [3] R. L. Merlino and J. Goree, *Phys. Today* **57**(7), 32 (2004).
 [4] P. K. Shukla and A. A. Mamun, *Introduction to Dusty Plasma Physics* (IOP, Bristol, 2002).
 [5] P. K. Shukla and B. Eliasson, *Rev. Mod. Phys.* **81**, 25 (2009).
 [6] R. Bharuthram and P. K. Shukla, *Planet. Space Sci.* **40**, 973 (1992).
 [7] S. I. Popel and M. Y. Yu, *Contrib. Plasma Phys.* **35**, 103 (1995).
 [8] P. K. Shukla and M. Rosenberg, *Phys. Plasmas* **6**, 1038 (1999).
 [9] Y. Nakamura, H. Bailung, and P. K. Shukla, *Phys. Rev. Lett.* **83**, 1602 (1999).
 [10] Q. Z. Luo, N. D'Angelo, and R. L. Merlino, *Phys. Plasmas* **7**, 3457 (1999).
 [11] Y. Nakamura and A. Sharma, *Phys. Plasmas* **8**, 3921 (2001).
 [12] A. A. Mamun and P. K. Shukla, *Phys. Plasmas* **9**, 1468 (2002).
 [13] A. A. Mamun and P. K. Shukla, *IEEE Trans. Plasma Sci.* **30**, 720 (2002).
 [14] R. Boström, *IEEE Trans. Plasma Sci.* **20**, 756 (1992).
 [15] P. O. Dovner *et al.*, *Geophys. Res. Lett.* **21**, 1827 (1994).
 [16] R. A. Cairns *et al.*, *Geophys. Res. Lett.* **22**, 2709 (1995).
 [17] A. A. Mamun, *Phys. Rev. E* **55**, 1852 (1997).
 [18] M. Tribeche and A. Berbri, *J. Plasma Phys.* **74**, 245 (2008).
 [19] J.-K. Xue, *Europhys. Lett.* **68**, 645 (2004).
 [20] M. Horányi, G. E. Morfill, and E. Grün, *Nature (London)* **363**, 144 (1993).
 [21] O. Havnes *et al.*, *J. Geophys. Res.* **101**, 10839 (1996).
 [22] V. E. Fortov *et al.*, *J. Exp. Theor. Phys.* **87**, 1087 (1998).
 [23] C. K. Goertz, *Rev. Geophys.* **27**, 271 (1989).
 [24] D. A. Mendis and M. Rosenberg, *Annu. Rev. Astron. Astrophys.* **32**, 419 (1994).
 [25] O. Havnes *et al.*, *Planet. Space Sci.* **44**, 1191 (1996).
 [26] S. Maxon and J. Viicelli, *Phys. Rev. Lett.* **32**, 4 (1974).